ISSN 2347-3487

A study of eutectic indium-bismuth and indium-bismuth-tin Field's metal rapidly solidified from melt

Mustafa Kamal[1], Abu-Bakr El-Bediwi[1], Rizk Mostafa Shalaby[1,*] Mohammed Younus[1,2]
[1] Metal Physics Lab. Physics Department Faculty of Science, Mansoura University, Mansoura, Egypt
kamal42200274@yahoo.com
baker_elbediwi@yahoo.com
*Corresponding author: doctorrizk2@yahoo.co.uk
Tel.: +2-01062507736
[2] On leave, M.Sc. student, Iraq
my_radi@live.com

Abstract

In this paper, the microstructure and thermal behavior of two rapidly solidified of eutectic Indium-Bismuth and Indium-Bismuth-Tin Field's metal are reported. This work experimentally measures the specific heat of the eutectic alloys of the binary Indium-bismuth and indium –bismuth –tin tertiary system using a differential scanning calorimeter (DSC) technique and analyzes the results to determine the thermodynamic properties of the system have sufficient scaling for experimental modeling applications. The resultant ribbons were studied by X-ray diffraction (XRD), scanning electron microscope (SEM) techniques, energy dispersive x-ray (EDX) technique. From the differential scanning calorimetry measurements, it is found that entropy change, enthalpy and specific heat are improved and enhanced compared with literature. The electrical resistivity was reported for temperatures between 295 and 330 K for all the melt-quenched ribbons of binary In-49Bi and tertiary In-32.5 Bi -16.5 Sn (wt.%). The microhardness, elastic moduli, internal friction and both thermal diffusivity and thermal effusivity were also measured. Field's metal is more than suitable for use in experimental settings as it is non-reactive, non-toxic, simple to manufacture, easy to use, and responds to a magnetic force.

Keywords

Field's metal; eutectic alloys; microstructure; thermal properties; rapid solidification technology.

Council for Innovative Research
Peer Review Research Publishing System
Journal: JOURNAL OF ADVANCES IN PHYSICS
Vol.7, No.2
www.cirjap.com, japeditor@gmail.com

ISSN 2347-3487

1. Introduction

Low melting point alloys, which typically contain indium, bismuth and tin, melt at temperatures less than 100C^{o}. These alloys are required for a wide variety of applications including: step soldering, thermal fuse application, rapid prototyping, die casting, mercury replacement, thermal cooling, heating designs and soft solder formulation. Determination of specific heat of eutectic indium- Bismuth- tin liquid metal alloys as a test material for liquid metal –cooled applications were studied by Adam Lipchitz et al. [1]. Recently, many countries are pursuing low melting alloys and liquid metal cooling applications as nuclear reactor coolants. The common liquid metal coolants considered for these cases are usually sodium, lead and lead-bismuth eutectic [1,2]; these designs use toxic materials at temperatures up to 1073 K for nuclear power plant operations and other similar applications. Use of these materials in academic laboratories is difficult due to the safety hazards. To investigate these systems in practical it requires a high level of safety systems. So, a less toxic and less reactive liquid metal must be used. The In–Bi–Sn ternary alloys have technologically importance in many applications such as nuclear reactor coolants material, die casting, rapid prototyping. These Alloys with eutectic composition may also consider as model alloys to investigate the pattern formation during solidification of eutectics [3-7]. Both of Bi and In, have great importance as main components of fusible alloys that also may be containing Ag, Sn, Zn and Sb, which is widely used in the electronic industry [8-10]. But specially, eutectic alloys of Bi–In–Sn ternary system have a wide range of fusible applications and are believed to be the most promising. the Bi–In system contains several intermetallics, i.e. the BiIn, Bi_3In_5,$BiIn_2$, that in contact with solid substrates, usually form a thin intermetallic compound layer, which is desirable to achieve a good metallurgical bond [11]. Kamal et al. have succeeded in producing sample of Sn-Bi-In by rapid solidification processing, in which tin-bismuth-indium melt-spun alloy containing two phases distributed uniformly with the Sn-matrix. On the bases of their observation, they prefer the Sn10Bi10In (wt. %) solder for intermediate step soldering in hermetic packaging [12]. Indium- -bismuth – Tin system has attracted attention in recent times because it has potential applications. There has been considerable scientific and technological interest in using rapid solidification processing, with cooling rates during solidification of >10^5 ks^{-1} to produce new structures and improved properties in a variety of metallic alloys. Thus the present study aims to contribute to a better understanding of the effect of rapid solidification on the structure and physical properties of eutectic In-Bi-Sn as Field's metal prepared by chill-block melt-spinning [13] to investigate the structural evolution with composition were as functional material.

2. Experimental techniques

The experimental techniques utilized have been described in details [2, 14-17] and will be repeated here only briefly. The materials used in the present work are In, Bi, and Sn granules, and the starting purity was better than 99.99 %. In-49Bi and tertiary In-32.5 Bi -16.5 Sn (wt.%) quenched from melt ribbons have been produced by a single aluminum roller coated with copper (200mm in diameter) melt-spinning technique[12]. The process parameters such as the ejection temperature and the linear speed of the wheel were fixed at 550 k and 30.4ms^{-1} respectively. The material flow rate Q_f has been empirically found to be an important chill block melt-spinning process variable and its dependence on readily adjustable apparatus parameters has been described by Liebermann [18] X-ray diffraction analysis was done on a Shimadzu x-ray diffractometer (DX-30), using Cu kα radiation (λ=1.5406Å) with Ni-filter. The microstructure analysis was carried out on a scanning electron microscope (SEM) of type (JEOL JSM-6510LV, Japan) operate at 30Kv with high resolution 3 nm. Differential thermal analysis (DTA) was carried out on a (SDT Q600, USA) with a heat rate 10^{o}C min^{-1}.The temperature dependence of resistivity was carried out by the double-bridge methods [19]. The variation of temperature during the resistance temperature investigation was determined using a step-down transformer connected to a constructed temperature control. The heating was kept constant during all the investigations at 5 K min^{-1} [14]. The elastic moduli, the internal friction and the thermal diffusivity of melt-spun ribbons were examined in air atmosphere with a modified dynamic resonance method [20]. The hardness of the melt-spun ribbons was measured using a digital Vickers microhardness tester (model FM-7), applying a load of 10 gf for 5 sec via a Vickers diamond pyramid [21]. More than fifteen indents were made on each sample to bring out any hardness variation due to the presence of more phases, so that the average value H_V would be obtained in melt In-49Bi and In-32.5 Bi -16.5 Sn (wt.%) quenched from melt ribbons.

3. Results and discussion

3. 1 Structural analysis

Rapid quenching of metallic alloys from melt was first carried out by Pol Duwez et al [22]. They found that the rapid quenching extends the solid solubility limits and produce non-equilibrium phase or amorphous alloys [23]. The diffraction patterns of these quenched ribbons disclosed the number and kind of phases at equilibrium or at non- equilibrium state in each melt spun ribbons. Fig (1a,b) produces an x-ray diffraction pattern of spun In-49Bi and In-32.5 Bi -16.5 Sn (wt.%) quenched from melt ribbons rapidly quenched from melt (500C^{o}), the pattern shows the existence of three kinds of phases ,In-phase and Sn-phase with tetragonal structure, Bi- phase with rhombohedral (hex) structure ,Ag-phase with cubic structure, also there was appearance of intermetallic compound BiIn peaks (tetragonal). A tetragonal crystal gives diffraction lines whose sin 2θ values satisfy the following equation, obtained by combining the Bragg law with the plane-spacing equation for the cubic system:

ISSN 2347-3487

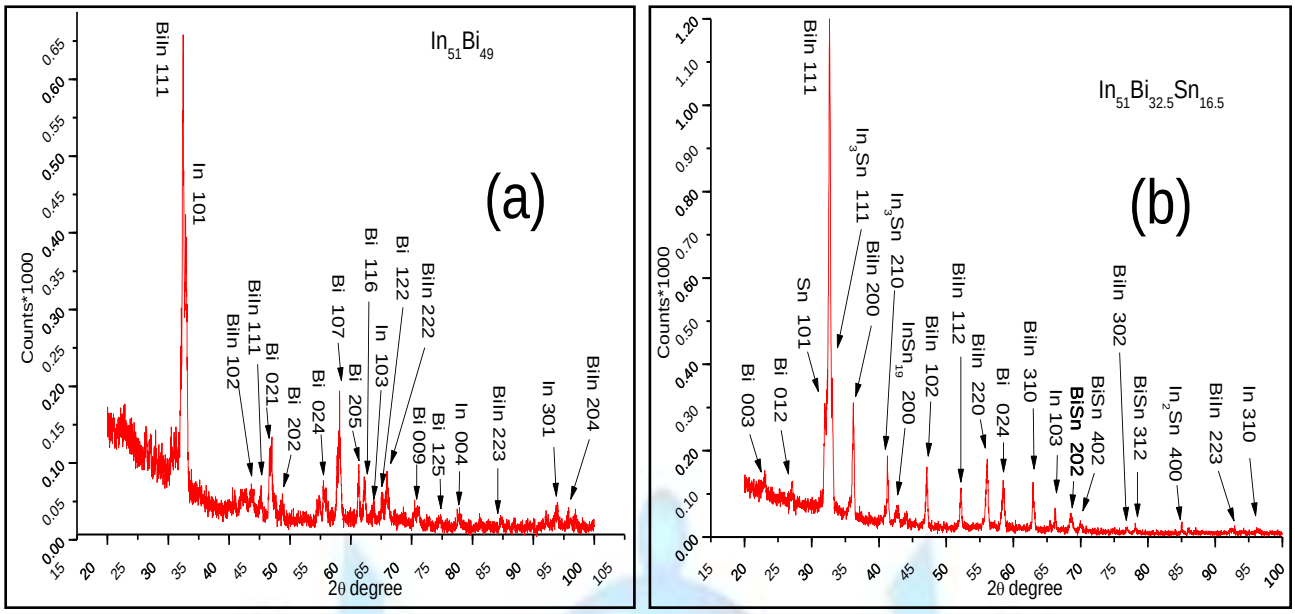

Figure 1 (a,b): X-ray diffraction pattern of eutectic In-49Bi and Field's metal alloys

$$\frac{1}{d^2} = \frac{h^2 + k^2}{a^2} + \frac{l^2}{c^2} \quad \ldots\ldots\ldots\ldots (1)$$

The lattice parameter, calculated from the sin2θ value for the highest-angle line, which indicated in table (1). Equation (1) predicts, for a particular incident wave length (λ) and a particular tetragonal cell of the unit cell size for this system involves two unknown parameters, a and c, all the possible Bragg angles at which diffraction occur from the planes (*hkl*) as indicated (for In phases) in the table (1).

Table 1: lattice parameters of eutectic In-Bi and Field's metal

System	a (Å)	c (Å)	c / a	Cell volume (Å^3)	Density (kg/m^3)
$In_{51}Bi_{49}$	3.2033	4.9465	1.5442	50.7561	6343.2342
$In_{51}Bi_{32.5}Sn_{16.5}$	3.2517	4.9813	1.5319	52.6691	5915.0204

The next step after identifying the phases of the unit cell is to find the number of atom in the unit cell (n). To find this number we use the fact that the volume of the unit cell (V), calculated from the lattice parameters multiplied by the measured density (ρ) of the melt-spun ribbons equals the weight of the all the atoms in the cell, for any crystal:

$$\rho = (\Sigma A) / N V \quad \ldots\ldots\ldots\ldots\ldots (2)$$

Where ΣA is the sum of the atomic weights of the atoms in the unit cell, If (V) in Equation (2) of a crystal is expressed in (Å^3) and the currently accepted value of Avogadro's number (N) inserted, then the equation (2) becomes

$$\sum A = \rho V / 1.66020 \quad \ldots\ldots\ldots\ldots (3)$$

$$\sum A = n A \quad \ldots\ldots\ldots\ldots\ldots (4)$$

Where n is the number of atom per unit cell.

Table 2: Number of atoms per unit cell

System	Number of atoms per unit cell
$In_{51}Bi_{49}$	1.1235
$In_{51}Bi_{32.5}Sn_{16.5}$	1.3777

The results listed in table (2), atoms are simply missing from a certain fraction of those lattice sites which they would be expected to occupy, and the result is non-integral number of atom per cell. This type of compound usually contains point defects and the distribution of point defects could have a short range order and it varies from cell to cell. If the crystallites

making up the specimen are sufficiently small, the maxima of the diffraction pattern are broadened by an amount inversely proportional to the crystallite size and measurement of the additional broadening thus gives a means of estimating the size through the formula given by Scherrer's [24] equation:

$$t = \frac{0.9\,\lambda}{B\,cos\theta_B} \qquad \ldots\ldots \qquad (5)$$

Where: B is the broadening of diffraction line measured at half its maximum intensity (radians) t is the diameter of crystal particle, θ_B is the Bragg angle and λ is the wave length of x-ray. This formula used to estimate the particle size of very small crystals from the measured width of their diffraction curves. In practic, a cell containing a non-integer umber of atoms as indicated in table (2), this type of cell usually contains point defects. We now look in detail at the sample broadening contribution. This arises from main sources known as crystallites size, lattice strains and stacking faults contribute to x-ray line broadening [25-27] **.**To derive information about the crystallite size (D_{eff}) and local lattice distortion (ε^2) in Indium phases:

$$B = \frac{1}{D_{eff}} + 5 < \varepsilon^2 >^{\frac{1}{2}} \frac{sin\theta}{\lambda} \qquad \ldots\ldots\ldots (6)$$

The $1/D_{eff}$ and $5 < \varepsilon^2 >^{½}$ are given in Table (3).

Table 3: Particle size and lattice distortion of eutectic In-49Bi and eutectic Field's metal

System	Particle size(Å)	$1/D_{eff}$ ($Å^{-1}$) $*10^{-3}$	$5<\sum^2>^{1/2} *10^{-3}$
$In_{51}Bi_{49}$	293.9437	3.4020	1.5586
$In_{51}Bi_{32.5}Sn_{16.5}$	212.9543	4.6958	1.5294

3.2 Microstructure

Microstructure of In-49Bi and eutectic Field's metal shown in Fig.2 (a,b). Generally, the microstructure of the high indium content is quite stable and do not obviously change during melt-spun process. This stability coupled with the lack of brittle intermetallic compounds (IMCs) in the matrix, makes high indium content used in a wide range of applications. The microstructure of In –Bi –Sn (IBS), alloys have apparently both light regions of coarse β-Sn grains and dark eutectic regions consists of mainly InBi intermetallic compound and β-Sn matrix, as shown in Fig.2 b.

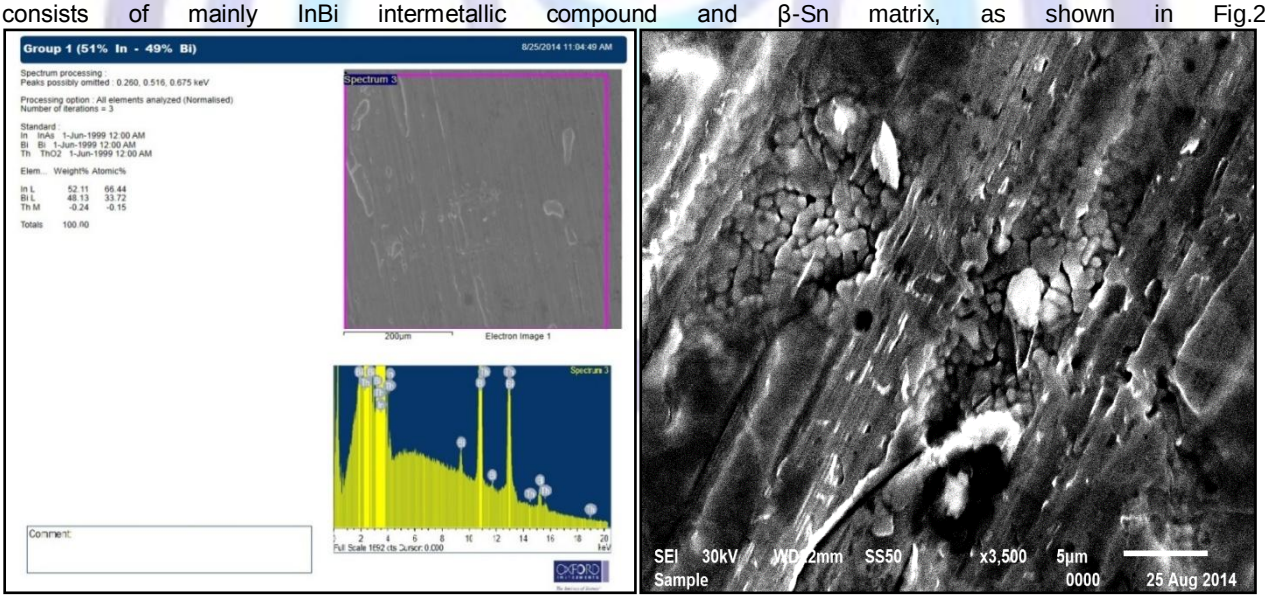

Figure 2 (a): EDX and SEM image for eutectic In-49Bi

(a)

ISSN 2347-3487

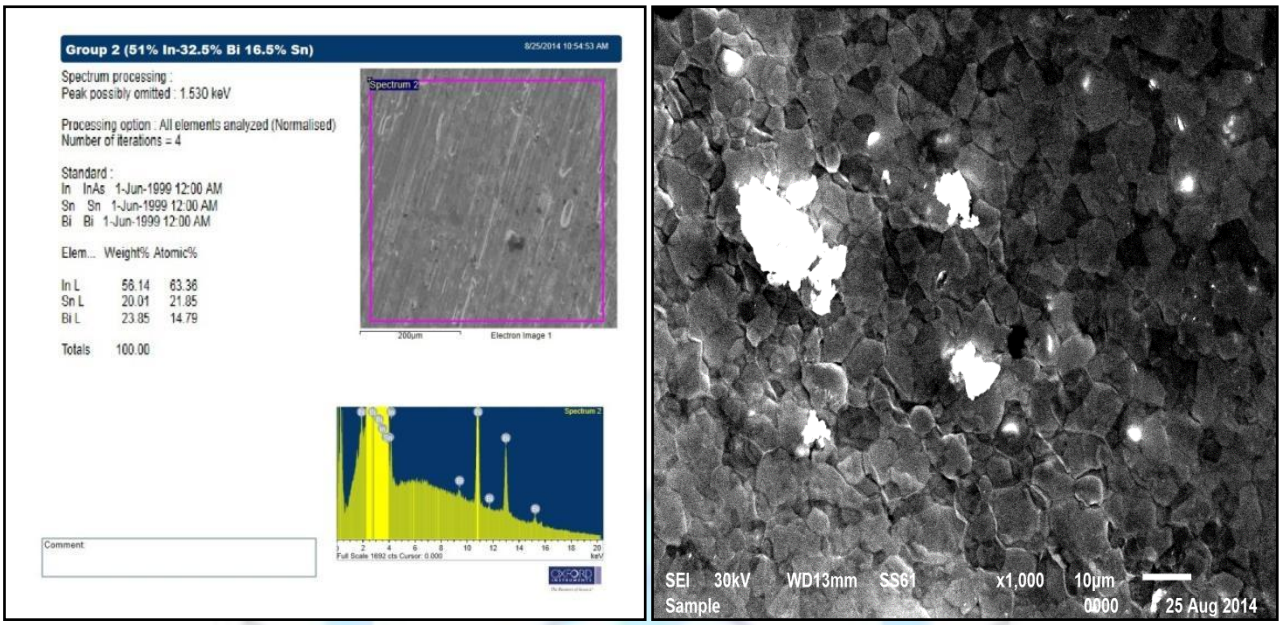

Figure 2(b): EDX and SEM image for eutectic Field's metal

3.3 Electrical resistivity and thermal conductivity

The rate of rise of electrical resistivity of a metal with temperature is dependent on the small amount of alloying present and on the state of deformation. The actual cause of resistivity must therefore be sought in deviations from the periodicity of the potential in which the electron move. It is on this concept that the modern theory of conductivity is based. Deviations from the periodicity of the potential causing resistivity maybe due to: (1) boundaries (2) lattice defects (3) lattice vibrations (4) foreign impurity atoms. The variation of electrical resistivity with the temperature in the range of 295- 330 K for In-49Bi and Field's metal alloys were measured and plotted as shown in Fig.(3). The values of (ρ) were found to be in the range of (1.7576) to (1.5997) and (1.5854) to (1.7248) µΩ.m for In-49Bi and Field's metal respectively. Fig.(3) shows that the resistivity increases linearly with the increasing temperature. This is because when the alloy is heated, thermal vibration increases.

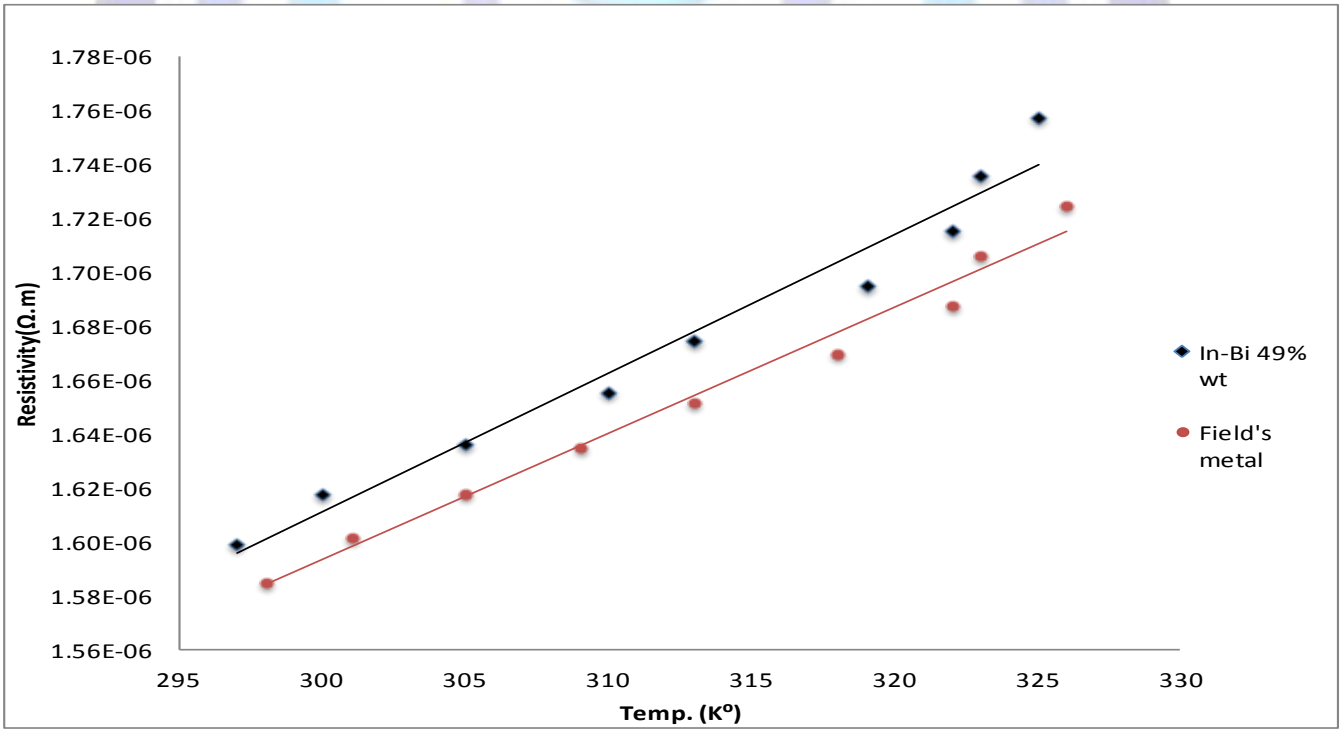

Figure 3: Variation of electrical resistivity with the temperature

Hence more vacancies are created leading to disordered in the periodicity, which diffracts and scatters the conduction electrons, thus reducing the conductivity. The measured electrical resistivity values of spun In_{51}-Bi_{49} and In_{51} -$Bi_{32.5}$ -$Sn_{16.5}$ (all in wt. percent) quenched from melt ribbons at around room temperature using double bridge method also temperature coefficient of resistivity values are shown in Table (4).

Table 4: Electrical properties of melt spun eutectic In-49 Bi and Field's metal

System	Resistivity $(\Omega.m)*10^{-6}$	Conductivity $(\Omega.m)^{-1}*10^{6}$	TCR $(K^{-1})*10^{-4}$
$In_{51}Bi_{49}$	1.7153	5.8297	12.500
$In_{51}Bi_{32.5}Sn_{16.5}$	1.6182	6.1799	12.610

The value of electrical conductivity (σ**)** accordingly to the quantum theory [28] is:

$$\sigma = \frac{ne^2\tau_F}{m} \quad \ldots\ldots (7)$$

The value of the collision time of an electron at the Fermi surface, (τ_F) may be calculated from equation (6) if conductivity is known where (*e,m*) are electron charge and mass respectively the. Typical values of (τ_F) are ≈10^{-14} sec. From an experimental measurement of σ of the as-melt quenched ribbons, we can use equation (6) estimate the values of the electron density (electrons/m^3) of the as-melt quenched ribbons. Tables (5,6) give the list of the transport parameters of the studied quenched ribbons from the melt. Values of the equivalent Fermi temperature T_f , Fermi energy E_f Fermi velocities v_f and Fermi wave numbr K_f are also given . Another important aspect of the electrical conduction process in general is that it enables us to compute the density of states at the Fermi surface Fs, g (E_f) within the framework of band theory [29], which leads finally to the following expression for the electrical conductivity:

$$\sigma = \frac{1}{3}e^2V_f^2\tau_f g(E_f) \quad \ldots\ldots\ldots\ldots\ldots (8)$$

Table 5: Transport parameters of eutectic In-49Bi and eutectic Field's metal

system wt%	Electron mobility μ $(m^2.V^{-1}.S^{-1})*10^{-3}$	Relaxation time τ $(sec)*10^{-14}$	Drift vilocity V_d (m /s)	Thermal conductivity $(w.m^{-1}.k^{-1})$	Electron specific heat $(J/kg^{-1}.K^{-1})$	number of free electrons(n) $m^{-3}*10^{26}$
$In_{51}Bi_{49}$	1.7604	1.0013	0.3878	4.3021	1.79272	2.0671
$In_{51}Bi_{32.5}Sn_{16.5}$	1.7604	1.0013	0.3878	4.5605	1.72435	2.1913

Table 6: Fermi parameters of eutectic In-49Bi and eutectic Field's metal

system wt%	Fermi wavenumber $(m^{-1})*10^{9}$	Fermi velocity $(m/s)*10^{5}$	Fermi energy (E_f) (ev)	Number of energy state $g(E_f)*10^{46}$	Fraction of excited electrons above fermi level$*10^{-2}$	Fermi Temperature $(K)*10^{3}$
$In_{51}Bi_{49}$	3.9409	4.5645	0.5918	3.2708	4.3984	6.8662
$In_{51}Bi_{32.5}Sn_{16.5}$	4.0183	4.6541	0.6152	3.3350	4.2306	7.1384

3.4 Thermal analysis

The melting temperature is a critical characteristic because it determines the maximum operating temperature of the system and the minimum processing temperature of the system and the minimum processing temperature which its components must survive. Melting temperature is a vital thermal property and has a strong influence on surface mount technology (SMT) field. Huang and Lee [30] were found that the onset point in the DSC heating curve represents the solidus temperature and that the peak point shows the liquidus temperature. Fig.4 (a,b) shows the DSC curves for In-49Bi and In -32.5Bi -16.5Sn (wt. %) quenched from melt ribbons . Zu et al. [31] suggested that structural changes take place to some extent in molten alloys as a function of temperature, which have been confirmed by the corresponding calorific peak in a differential scanning calorimeter. So in this section, it is noted that further work is needed to probe the concrete change of structures with the help of a differential scanning calorimeter. Specimens approximately 7 mg in mass were cut from the melt-spun ribbons and were submitted to heating from room temperature to about 350 C^o at rates of 10 $K.min^{-1}$ in

ISSN 2347-3487

a SDTQ600 differential scanning calorimeter (DSC). A typical output is depicted in Fig. 3(a, b). The results of the solidus and liquidus temperature, melting temperature, pasty range, enthalpy, entropy change and the average specific heat are tabulated in Table (7).

Table 7: Thermal analysis of eutectic In-49Bi and Field's metal.

System	T_s (k^o)	T_m (k^o)	T_l (k^o)	pastry range (k^o)	Enthalpy H (j/g)	Specific heat C_p (j/g.k)	Entropy change S (j/g.k)
In_{51}-Bi_{49}	333	341.21	352	19	78.81	4.148	230.203
In_{51}-$Bi_{32.5}$-$Sn_{16.5}$	325	333.34	337	12	51.62	4.302	155.997

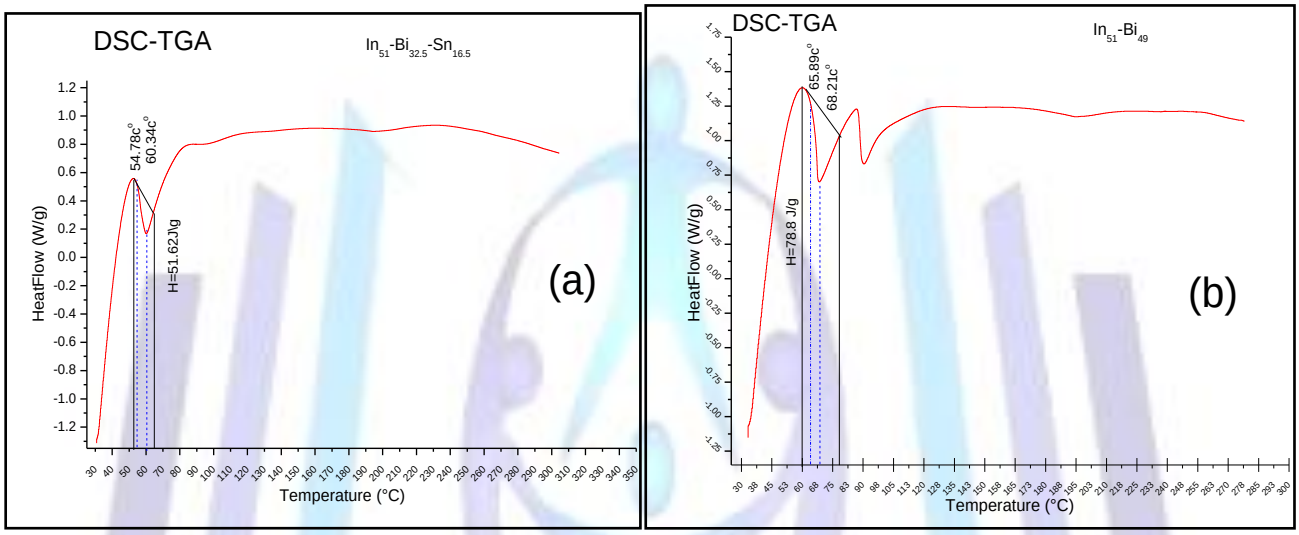

Figure 4: Deferential scanning calorimetry of rapidly solidified, a) In-49Bi, b) Field's metal.

3.4.1Thermal diffusivity and thermal effusivity

In heat transfer analysis, thermal diffusivity is the thermal conductivity (k) divided by density (ρ) and specific heat capacity (c_p) at constant pressure [32]. It measures the ability of a material to conduct thermal energy relative to its ability to store thermal energy. It has the SI unit of m²/s. Thermal diffusivity is usually denoted (D_{th}). The formula is:

$$D_{th} = \frac{k}{\rho c_p} \ldots\ldots\ldots\ldots\ldots (9)$$

Thermal diffusivity is the ratio of the time derivative of temperature to its curvature, quantifying the rate at which temperature concavity is "smoothed out". In a sense, thermal diffusivity is the measure of thermal inertia in a substance with high thermal diffusivity, heat moves rapidly through it because the substance conducts heat quickly relative to its volumetric heat capacity or (thermal bulk) [33]. The importance of thermal conductivity and for thermal diffusivity is associated with the need for appreciable levels of thermal conductance in soldering process The information on these parameters of In-49Bi and In-32.5 Bi-16.5 Sn (wt. %) quenched from melt ribbons is necessary for modeling the optimum conditions during processing, as well as for an analysis for transport of heat in (In-Bi-Sn) melt-spun ribbons during practical applications. Using dynamic resonance technique and from the frequency f_o, at which peak damping occurs, the thermal diffusivity D_{th} can be obtained from the:

$$D_{th} = \frac{2t^2 f_o}{\pi} \ldots\ldots\ldots\ldots\ldots (10)$$

Table 8: Thermal diffusivity and thermal effusivity of eutectic In-49Bi and

System	Thermal Diffusivity $(m^2/s)*10^{-7}$	Thermal Effusivity $(js^{-1/2}m^{-2}k^{-1})$
$In_{51}Bi_{49}$	0.9723	10.6392
$In_{51}Bi_{32.5}Sn_{16.5}$	1.4443	10.7722

Where, t is the thickness of the quenched ribbons. The thermal effusivity is a relevant thermophysical parameter for surface heating or cooling process as well as in quenching process. The effusivity of a material is the square root of the product of the thermal conductivity, density and heat capacity.

$$E_{th} = \sqrt{k.\rho.c_p} \quad \dots\dots\dots\dots\dots\dots (11)$$

The units are a little strange ($j.s^{-1/2}m^{-2}k^{-1}$). The effusivity measures the rate at which a material can absorb heat. The effusivity of your hand and the object it touches determines the surface temperature of your hand. Since both of your hands have the same effusivity, it is the effusivity of the materials you touch that causes you to feel different surface temperatures in your hands. If the effusivity of a material is high, like for metals, the interfacial temperature is lower when touching the cold metal because the material can absorb and transport heat away from your hand much faster. Table (8) summarized the values of thermal diffusivity and thermal effusivity for quenched ribbons. The value of thermal diffusivity of quenched ribbons controls the time rate of temperature change as heat passes through quenched ribbons. So it is a measure of the rate at which a body with a nonuniform temperature reaches a state of thermal equilibrium.

3.5 Mechanical behavior and microhardness

The dynamic resonance method has a definite advantage over static method of measuring elastic moduli because the low-level alternating stress does not inflate anelastic processes such as creep or elastic hysteresis [34]. The elastic moduli obtained with the resonance method give information about elastic compliances along the long axis of the melt-spun ribbons. In an elastically isotropic body such as a well prepared polycrystalline quenched ribbons, the elastic moduli are identical in any direction. Elastic moduli can be obtained from frequency f_o, at which peak damping occurs, according to:

$$E = \frac{38.32\rho l^4 f_0^2}{t^2} \quad \dots\dots\dots\dots\dots\dots (12)$$

$$G = \frac{E}{2(1+\nu)} \dots\dots\dots\dots\dots\dots\dots (13)$$

$$B = \frac{E}{3(1-2\nu)} \quad \dots\dots\dots\dots\dots\dots\dots (14)$$

Where, (E) is elastic modulus (Young's modulus), (ρ) is ribbon density, (l) is vibrated part of ribbon, t is ribbon thickness, G is share modulus, B is bulk modulus and v is poison's ratio. Another important characteristic of melt-spun ribbons can be calculated from frequency f_o, at which peak damping occurs which is internal friction (Q^{-1}). Internal friction measurements have been quite fruitful for learning the behavior of rapidly quenched ribbons from melt. It is one of the important characteristics which are indirectly related to their elastic properties. The free vibration is based on the measurement of the decay in amplitude of vibrations during free vibration. The internal friction is obtained by [35]:

$$Q^{-1} = 0.5773\left(\frac{\Delta f}{f_o}\right) \quad \dots\dots\dots (15)$$

Also we investigate the microhardness (H_v) of quenched ribbons Values of young modulus E, shear modulus G and bulk modulus B Poisson's ratio internal friction microhardness result of $In_{51}Bi_{49}$ and $In_{51}Bi_{32.5}Sn_{16.5}$ (all in wt. percent) quenched from melt ribbons listed in table (9).

Table 9: Mechanical properties of eutectic In-49Bi and eutectic Field's metal.

System	Young's modulus (GPa)	Shear modulus (Gpa)	Bulk modulus (GPa)	Poisson's ratio	Q^{-1}	Hardness (MPa)
$In_{51}Bi_{49}$	12.5982	4.7733	11.6424	0.3197	0.0301	187
$In_{51}Bi_{32.5}Sn_{16.5}$	14.4375	5.4908	12.9857	0.3147	0.0303	175

Conclusion:

In the present work, the influence of solidification processing parameter on the structural, thermal, electrical and mechanical properties of In-49Bi binary eutectic alloy and In-32.5Bi-16.5Sn ternary alloy were investigated. The results are summarized as follows:

1- From microstructure examination, the BiIn IMC is precipitated within the β-Sn matrix in the In-49Bi alloy. The ternary In-32.5Bi-16.5Sn Field's metal exhibited additional In_3Sn, $InSn_{19}$, and BiSn IMCs phases. The IMCs particles contributed to a dispersion strengthening effect to the In-Bi-Sn alloy.

2- Rapidly solidified In-49Bi and In-32.5Bi-16.5Sn Field's metal exhibited superior combination of mechanical properties and thermal properties when compared with commercially available alloys.

3- The electrical resistivity of In-49 Bi eutectic alloy increased from 1.599 μΩ.m to 1.758 μΩ.m by increasing temperature compared to In-32.5Bi-16.5Sn Field's metal increased from 1.586 μΩ.m.to 1.725 μΩ.m.

4-The values of the enthalpy of fusion and the specific heat for In-49 Bi and In-32.5Bi-16.5Sn were found to be 78.81(J/g), 4.148 (J/g.K) and 51.62(J/g), 4.302 (J/g.K) respectively.

5- By using chill-block melt spinning technique at cooling rate $\approx 10^5$ Ks^{-1}, the grain size of the ribbons decreases greatly because of the reduced solidification time prior to solidification. Due to the strength of grain size, the elastic moduli and microhardness increases.

6- Rapid solidification provides a ribbon with refined microstructure grains of about 30 nm.

References

[1] Lipchitz A., Harve G. l, Sunagawa T. Applied Mechanics and Materials, Vol. 420 (2013) pp.185

[2] Kamal M., El-Bediwi A., Majeed J. K. IJET-IJENS Vol: 14 No: 02 pp. 5-15 April 2014

[3] Witusiewicz V.T., Hecht U., Böttger B., Rex S. Journal of Alloys and Compounds Volume 428, Issues 1–2, 31 January 2007, Pages 115–124

[4] Witusiewicz V.T., Hecht U., Rex S., M. Apel Acta Mater, 53 (2005), pp. 3663–3669

[5] Rex S., Böttger B., Witusiewicz V., Hecht U. Mater. Sci. Eng. A, 413–414 (2005), pp. 249–254,

[6] Ruggiero M.A., Rutter J.W., Mater. Sci. Technol., 11 (1995), pp. 136–142

[7] Ruggiero M.A., Rutter J.W. Mater., Sci. Technol., 13 (1997), pp. 5–11

[8] Frear D.R., Jang J.W., Lin J.K., Zhang C., JOM, 53 (6) (2001), pp. 28–32,

[9] Yoon S.W., Soh J.R, Lee H.M., Lee B.-J., Acta Mater, 45 (3) (1997), pp. 951–960

[10] Yamaguchi A., Yamashita Y., Furusawa A., Nishida K., Hojo T., Sogo Y., Miwa R., Hirose A., Kobayashi K.F., Japan Inst. Metals, 69 (1) (2005), pp. 139–146.

[11] Gnecco F., Ricci E., Amore S., Giuranno D., Borzone G., Zanicchi G., Novakovic Adhes R. J., Adhesives, 27 (2007), pp. 409–416

[12] Kamal M., El-Bediwi A.,Badr sh.,Taha S. IJET-IJENS Vol: 12 No: 03 pp. 6-11 (2012).

[13] Kamal M. and Mohamed U. S., A Review Chill-Block Melt spin Technique, Theoretical and Applications, eISBN: 978-1- 608005-151-9(2012), Bentham eBooks.

[14] Kamal M., El-Bediwi A. and El-Ashram T., Journal of Materials science in Electronics 15(2004) 211-217.

[15] Shalaby R. M. and Kamal M., International Journal of physic and Research (IJPR), Vol.13, Issues, Dec. (2013), 51-60.

[16] Kamal M., Badr Sh. and Abdelhakim N. A., International Journal of Engineering and Technology IJET-IJENS Vol: 14, No: 01 Feb. (2014) IJENS, PP:119-129.

[17] Kamal M., Shaban A.M., El-Kady M., Shalaby R.M., Radiation effects and defects in solids, 138, (1996)307-318.

[18] Liebermann H. H., Materials Science and Engineering, 43 (1980) 203-210.

[19] Geller Y.A., A. Rakhshtadt G., "Science of Materials", Mir publishers, Moscow, 1977, P. 138.

[20] Shaban A.M. and Kamal M., Radiation Effects and Defects in Solids, (1995), Vol.133, PP: 5-13.

[21] Kamal M., El-Bediwi A., Radiation Effects and Defects in solids 174(1999)211.

[22] Duwez Pol, Willens R. H., and Klement W. Jr., J. Appl. Phys.31, 1137(1960)

[23] Duwez Pol and Willens R.H,Trans.Met .Soc. AIME 227 , 326 (1963) .

[24] CULLITY B. D., Elements of X-ray Diffraction (second edition). Addison-Wesley publishing company. (1978)

[25] Lain E.S.U,Hiltune E.J,Heinonen. Acta Metallurgica vol. 28, PP1565-1569 (1980)

[26] Manaila R., Zavalche F., Popescu R., Macovei D., Devenyi A., Bunescu C., Vasile E. and Jianu A. Materials science and engineering A 226-228 (1997) 290-295

[27] Williamson G.K. and Hall W.H., Acta Metallurgy, vol. 1, Jan. 1953, 22-31

[28] Kamal M., El-Bediwi A., Journal of Materials science: Material in Electronics 11(2000)519- 523.

[29] Omar M.A., Elementary solid state physics; principles and Application, Addison-Wesley publishing company, 1975 PP: 235-238.

[30] Huang B., Lee N.C., Int. Symp. Microelectron. Proc. 3906 (1999) 711.

[31] Zu F.Q., Zhu Z. G., Zhang B., Feng Y. and Shui J.P., J. phys. Condens. Matter 13 (2001) 11435-11442

[32] Lide, David R., ed. (2009). CRC Handbook of Chemistry and Physics (90th ed.). Boca Raton, Florida: CRC Press. p. 2-65.

[33] Venkanna B.K. (2010). Fundamentals of Heat and Mass Transfer. New Delhi: PHI Learning. p. 38. ISBN 978-81-203-4031-2. Retrieved 1 December 2011

[34] Schreiber E., Anderson O. L., and Soga N., Elastic Constants and their Measurements, McGraw-Hill Book Company (1973) PP: 82-125

[35] Roebbon G., Bollen B., Brebels A., Humbeeck J. Van and Van der Biest O., Rev. Sci. Instrum. 68(12), December (1997), Americam Institute of physics PP: 4511-4515.